Density functional perturbation theory within the projector augmented wave method

Andrea Dal Corso
International School for Advanced Studies (SISSA), Via Beirut 2/4, I-34151 Trieste, Italy
and IOM-DEMOCRITOS, Trieste, Italy

(Received 12 December 2008; revised manuscript received 29 January 2010; published 25 February 2010)

Density functional perturbation theory (DFPT) with ultrasoft pseudopotentials (US-PPs) is extended to the projector augmented wave (PAW) method. I show that minor modifications of the existing DFPT codes for US-PPs are sufficient for dealing with PAW. A few applications to small molecules (CO, H_2O) and to ferromagnetic Fe in the body-centered cubic structure validate the theory.

DOI: 10.1103/PhysRevB.81.075123 PACS number(s): 71.15.Dx, 63.10.+a

I. INTRODUCTION

Among the *ab initio* methods for calculating the linear response properties of solids such as phonons, dielectric constants, or Born effective charges (BEC), density functional perturbation theory (DFPT) stands out as one of the most widespread, due to its efficiency and accuracy.[1] Originally implemented with plane waves and semilocal pseudopotentials (PPs),[2] DFPT is now available within both all-electron[3,4] and PP schemes based on fully separable norm conserving (NC) (Refs. 1, 5, and 6) or ultrasoft (US) PPs.[7–9] Plane waves and PPs are quite attractive mainly for their computational efficiency. However, PPs introduce a small transferability error (TE) that makes the numerical results slightly dependent on the details of the PP construction. In recent years, some applications have highlighted the importance of reducing the TE and to increase accuracy.[10,11] The comparison of different functionals for the exchange and correlation energy on the properties of molecules[10] and solids[11] requires quite small TEs. Moreover, it might happen that the TE hides interesting physical effects. A paradigmatic example is the effect of magnetism or of spin-orbit coupling on the phonon frequencies.[9,12] The frequency changes expected in these cases are sometimes comparable to the differences found using different PPs. In order to deal with these situations, it could be useful to apply the projector augmented wave (PAW) method which is based on plane waves but is, in principle, equivalent to a frozen-core all-electron method.[13] Actually, both the US-PPs and the NC-PPs are well defined approximations of the PAW method[13,14] and numerically, it has been proved that the PAW TEs are often smaller than those of the other PPs, especially in magnetic systems.[14] In previous years, I generalized DFPT in order to deal with US-PPs.[8,9] Recently, Audouze *et al.* derived DFPT within the PAW scheme[15,16] and compared their final expressions with Ref. 8. So far, however, they have not shown any application of these formulas. In this paper, I give different expressions for DFPT in the PAW case and discuss the US-PPs approximation. In particular, DFPT in the PAW case is written as a minor addition to the US-PPs expressions so that these formulas are simpler to implement on a code where DFPT with US-PPs is already available. I validate the theory in a few cases: two molecules (CO and H_2O) and bcc-Fe. In these examples, the new terms give small, but not totally negligible, corrections to the calculated vibrational frequencies.

II. THEORY

In the PAW approach to density functional theory, the frozen-core total energy of a gas of N electrons in the field of fixed ions at positions $\mathbf{R}_I$ is a functional of the pseudowave functions $\tilde{\psi}_{i,\sigma}$ (here, i indicates the occupied states and σ indicates the spin index). Within the local spin density approximation, the frozen-core energy is calculated by a PAW transformation[13] of the all-electron frozen-core energy, with the help of all-electron ($|\Phi_n^{I,AE}\rangle$) and pseudo ($|\Phi_n^{I,PS}\rangle$) partial waves and projector functions ($|\beta_n^I\rangle$). Quantities varying rapidly close to the nuclei are calculated on radial grids introducing a sphere about each atom, while smoother quantities are calculated on a real space mesh or, equivalently, in reciprocal space by a Fourier transformation. We refer to Refs. 13 and 14 for a detailed discussion. Here, we start from the PAW expressions of the total energy, of the Hamiltonian and of the Hellmann-Feynman forces given in Ref. 14, although for a few quantities we use a notation closer to Ref. 8. The US and PAW charge densities calculated on the real space mesh, $\tilde{\rho}_\sigma+\hat{\rho}_\sigma$, have the same expression and they are given with Eqs. (3) and (4) in Ref. 8.[17] In the PAW scheme, additional charge densities are defined within the spheres about each atoms: $\rho_\sigma^{1,I}$ and $\tilde{\rho}_\sigma^{1,I}+\hat{\rho}_\sigma^I$. They are given by Eqs. (5), (6), and (27) in Ref. 14. In our notation, we have

$$\rho_\sigma^{1,I}(\mathbf{r}) = \sum_{mn} \langle \Phi_m^{I,AE}|\mathbf{r}\rangle\langle\mathbf{r}|\Phi_n^{I,AE}\rangle \rho_{mn}^{I,\sigma}, \tag{1}$$

where $\rho_{mn}^{I,\sigma}=\Sigma_i\langle\tilde{\psi}_{i,\sigma}|\beta_m^I\rangle\langle\beta_n^I|\tilde{\psi}_{i,\sigma}\rangle$ (the sum over i is on occupied states). $\tilde{\rho}_\sigma^{1,I}+\hat{\rho}_\sigma^I$ are given by Eq. (1) with $\langle\Phi_m^{I,AE}|\mathbf{r}\rangle\langle\mathbf{r}|\Phi_n^{I,AE}\rangle$ substituted by $\langle\Phi_m^{I,PS}|\mathbf{r}\rangle\langle\mathbf{r}|\Phi_n^{I,PS}\rangle + \hat{Q}_{mn}^I(\mathbf{r})$.[18] This replacement is used several times in the following and we call it all-electron pseudo (AE-PS) substitution. The frozen-core total energy of the electron gas can be written as $E_{\rm tot}=\tilde{E}+E^1-\tilde{E}^1$, where $\tilde{E}$ is calculated on the real space mesh while E^1 and $\tilde{E}^1$ are calculated on the spheres. With our notation, Eq. (21) of Ref. 14 becomes (in Hartree a.u.)

$$\tilde{E} = \sum_{i,\sigma} \langle\tilde{\psi}_{i,\sigma}| -\frac{1}{2}\nabla^2|\tilde{\psi}_{i,\sigma}\rangle + E_{xc}[\{\tilde{\rho}_\sigma+\hat{\rho}_\sigma+\tilde{\rho}_{c,\sigma}\}] + E_H[\tilde{\rho}+\hat{\rho}] + \int d^3r \tilde{V}_{\rm loc}(\mathbf{r})[\tilde{\rho}(\mathbf{r})+\hat{\rho}(\mathbf{r})] + U_{I,I}. \tag{2}$$

For each atom, we call local potential, $\tilde{v}^I_{\rm loc}(\mathbf{r})$, the quantity that in Ref. 14 is indicated with $v_H(\tilde{n}^I_{\rm Zc})$. $\tilde{v}^I_{\rm loc}(\mathbf{r})$ coincides with the all-electron local potential $v^I_{\rm loc}(\mathbf{r})=v_H(n^I_{\rm Zc})$ outside the spheres. Moreover, we define the local potential in the real space mesh as: $\tilde{V}_{\rm loc}(\mathbf{r})=\Sigma_I\tilde{v}^I_{\rm loc}(\mathbf{r}-\mathbf{R}_I)$. $\tilde{\rho}(\mathbf{r})+\hat{\rho}(\mathbf{r})$ is the sum of the two spin components. The core charges are defined as in Ref. 14 and are spin unpolarized: $\tilde{\rho}_{c,\sigma}(\mathbf{r})=1/2\tilde{\rho}_c(\mathbf{r})$ with similar relationships holding for the other core charges. $U_{I,I}$ is the ion-ion interaction energy dealt with by Ewald techniques.[19] With these notations, Eq. (22) of Ref. 14 becomes

$$\tilde{E}^1=\sum_{I,mn,\sigma}\rho^{I,\sigma}_{mn}\langle\Phi^{I,PS}_m|-\frac{1}{2}\nabla^2|\Phi^{I,PS}_n\rangle+\sum_I E_{xc}[\{\tilde{\rho}^{1,I}_\sigma+\hat{\rho}^I_\sigma+\tilde{\rho}^I_{c,\sigma}\}]+\sum_I E_H[\tilde{\rho}^{1,I}+\hat{\rho}^I]+\sum_I\int_{\Omega_I}d^3r\tilde{v}^I_{\rm loc}(\mathbf{r})[\tilde{\rho}^{1,I}(\mathbf{r})+\hat{\rho}^I(\mathbf{r})],\tag{3}$$

while Eq. (23) of Ref. 14 becomes

$$E^1=\sum_{I,mn,\sigma}\rho^{I,\sigma}_{mn}\langle\Phi^{I,AE}_m|-\frac{1}{2}\nabla^2|\Phi^{I,AE}_n\rangle+\sum_I E_{xc}[\{\rho^{1,I}_\sigma+\rho^I_{c,\sigma}\}]+\sum_I E_H[\rho^{1,I}]+\sum_I\int_{\Omega_I}d^3rv^I_{\rm loc}(\mathbf{r})\rho^{1,I}(\mathbf{r}).\tag{4}$$

The minimization of the total energy with respect to the pseudowave functions, which obey the generalized orthogonality constraint $\langle\tilde{\psi}_{i,\sigma}|S|\tilde{\psi}_{j,\sigma}\rangle=\delta_{i,j}$, gives the Kohn and Sham equations: $H^\sigma|\tilde{\psi}_{i,\sigma}\rangle=\varepsilon_{i,\sigma}S|\tilde{\psi}_{i,\sigma}\rangle$ with an Hamiltonian[14]

$$H^\sigma=-\frac{1}{2}\nabla^2+\int d^3r\tilde{V}^\sigma_{\rm eff}(\mathbf{r})K(\mathbf{r})+\sum_{I,mn}(D^{1,\sigma}_{I,mn}-\tilde{D}^{1,\sigma}_{I,mn})|\beta^I_m\rangle\langle\beta^I_n|,\tag{5}$$

where $K(\mathbf{r})$ is defined in Eq. (5) of Ref. 8 and

$$D^{1,\sigma}_{I,mn}=\int_{\Omega_I}d^3r\Phi^{I,AE}_m(\mathbf{r})\left(-\frac{1}{2}\nabla^2\right)\Phi^{I,AE}_n(\mathbf{r})+\int_{\Omega_I}d^3r\Phi^{I,AE}_m(\mathbf{r})\Phi^{I,AE}_n(\mathbf{r})V^{I,\sigma}_{\rm eff}(\mathbf{r}),\tag{6}$$

where Ω_I indicates the volume of the sphere about the atom I. $\tilde{V}^\sigma_{\rm eff}(\mathbf{r})$ is the sum of the local, Hartree and exchange and correlation potentials: $\tilde{V}^\sigma_{\rm eff}(\mathbf{r})=\tilde{V}_{\rm loc}(\mathbf{r})+V_H[\tilde{\rho}(\mathbf{r})+\hat{\rho}(\mathbf{r})]+V^\sigma_{xc}[\{\tilde{\rho}_\sigma(\mathbf{r})+\hat{\rho}_\sigma(\mathbf{r})+\tilde{\rho}_{c,\sigma}(\mathbf{r})\}]$. $V^{I,\sigma}_{\rm eff}$ and $\tilde{V}^{I,\sigma}_{\rm eff}$ are calculated as $\tilde{V}^\sigma_{\rm eff}(\mathbf{r})$ using the corresponding charge densities and local potentials. $\tilde{D}^{1,\sigma}_{I,mn}$ is given by Eq. (6), putting the partial waves $\Phi^{I,PS}_k(\mathbf{r})$ in the place of $\Phi^{I,AE}_k(\mathbf{r})$ ($k=m$ or $k=n$) in the first integral, $\tilde{V}^{I,\sigma}_{\rm eff}(\mathbf{r})$ in the place of $V^{I,\sigma}_{\rm eff}(\mathbf{r})$ in the second, and making an AE-PS substitution in the second integral. $D^{1,\sigma}_{I,mn}$ and $\tilde{D}^{1,\sigma}_{I,mn}$ are calculated on the spheres about each atom. When an atom moves, $D^{1,\sigma}_{I,mn}$ and $\tilde{D}^{1,\sigma}_{I,mn}$ change because the charge densities $\rho^{1,I}_\sigma$ and $\tilde{\rho}^{1,I}_\sigma+\hat{\rho}^I_\sigma$ change. Note, however, that the partial waves, the core charges or the local potentials inside the spheres, do not change. Actually, these quantities are calculated with respect to the position of the atom and are displaced rigidly. Moreover, $\hat{Q}^I_{mn}(\mathbf{r})$ has the same dipole moments as the difference $\langle\Phi^{I,AE}_m|\mathbf{r}\rangle\langle\mathbf{r}|\Phi^{I,AE}_n\rangle-\langle\Phi^{I,PS}_m|\mathbf{r}\rangle\langle\mathbf{r}|\Phi^{I,PS}_n\rangle$ so that, for an electric field perturbation, the contribution of the change in the local potential inside the spheres vanishes. The US-PP formalism is a particular case of the PAW formalism in which the two energies E^1 and $\tilde{E}^1$ calculated inside the spheres and dependent on the occupancies $\rho^{I,\sigma}_{mn}$, are linearized around the atomic reference occupancies.[14] Therefore, in the US case, $D^{1,\sigma}_{I,mn}$ and $\tilde{D}^{1,\sigma}_{I,mn}$ are kept constant and calculated on isolated atoms neglecting spin polarization. Their difference is equal to the unscreened nonlocal US-PPs coefficients: $D^{(0),\gamma(I)}_{mn}=D^{1,\sigma}_{I,mn}-\tilde{D}^{1,\sigma}_{I,mn}$.

Let us now consider the first order derivative of the charge densities with respect to an external parameter μ that, to fix the ideas, might be an atomic displacement[8] or a component of the electric field present within the system.[20] The US and PAW derivatives of $\tilde{\rho}_\sigma+\hat{\rho}_\sigma$ are equal and given by Eq. (28) in Ref. 8

$$\frac{d[\tilde{\rho}_\sigma(\mathbf{r})+\hat{\rho}_\sigma(\mathbf{r})]}{d\mu}=2\,\mathrm{Re}\sum_i\langle\tilde{\psi}_{i,\sigma}|K(\mathbf{r})|\Delta^\mu\tilde{\psi}_{i,\sigma}\rangle-\sum_i\langle\tilde{\psi}_{i,\sigma}|K(\mathbf{r})\times|\delta^\mu\tilde{\psi}_{i,\sigma}\rangle+\sum_i\langle\tilde{\psi}_{i,\sigma}|\frac{\partial K(\mathbf{r})}{\partial\mu}|\tilde{\psi}_{i,\sigma}\rangle.\tag{7}$$

$|\Delta^\mu\tilde{\psi}_{i,\sigma}\rangle=\tilde{P}_{c,\sigma}|\frac{d\tilde{\psi}_{i,\sigma}}{d\mu}\rangle$, where $\tilde{P}_{c,\sigma}$ is the projector in the conduction band, and $|\delta^\mu\tilde{\psi}_{i,\sigma}\rangle=\Sigma_j|\tilde{\psi}_{j,\sigma}\rangle\langle\tilde{\psi}_{j,\sigma}|\frac{\partial S}{\partial\mu}|\tilde{\psi}_{i,\sigma}\rangle$. For the following, it is convenient to call $\Delta^\mu[\tilde{\rho}_\sigma(\mathbf{r})+\hat{\rho}_\sigma(\mathbf{r})]$ the last two terms of Eq. (7). $\rho^{1,I}_\sigma$ and $\tilde{\rho}^{1,I}_\sigma+\hat{\rho}^I_\sigma$ are allowed to change in the PAW scheme only and their derivatives are given by

$$\frac{d\rho^{1,I}_\sigma(\mathbf{r})}{d\mu}=\sum_{mn}\langle\Phi^{I,AE}_m|\mathbf{r}\rangle\langle\mathbf{r}|\Phi^{I,AE}_n\rangle\frac{d\rho^{I,\sigma}_{mn}}{d\mu},\tag{8}$$

where

$$\frac{d\rho^{I,\sigma}_{mn}}{d\mu}=\sum_i(\langle\tilde{\psi}_{i,\sigma}|\beta^I_m\rangle\langle\beta^I_n|\Delta^\mu\tilde{\psi}_{i,\sigma}\rangle+\langle\Delta^\mu\tilde{\psi}_{i,\sigma}|\beta^I_m\rangle\langle\beta^I_n|\tilde{\psi}_{i,\sigma}\rangle)+b^{\sigma,\mu}_{I,mn},\tag{9}$$

and

$$b^{\sigma,\mu}_{I,mn}=\sum_i\langle\tilde{\psi}_{i,\sigma}|\frac{\partial(|\beta^I_m\rangle\langle\beta^I_n|)}{\partial\mu}|\tilde{\psi}_{i,\sigma}\rangle-\sum_i\langle\tilde{\psi}_{i,\sigma}|\beta^I_m\rangle\langle\beta^I_n|\delta^\mu\tilde{\psi}_{i,\sigma}\rangle,\tag{10}$$

$b^{\sigma,\mu}_{I,mn}$, as well as the first term in Eq. (9), are quantities needed also in the US scheme to calculate $\frac{d\hat{\rho}_\sigma}{d\mu}$, and Eq. (8) is similar to Eq. (1), thus it can be calculated by the same routine. Similarly, $\frac{d(\tilde{\rho}^{1,I}_\sigma+\hat{\rho}^I_\sigma)}{d\mu}$ can be calculated as $\frac{d\rho^{1,I}_\sigma}{d\mu}$ with an AE-PS substitution. Note that with respect to the expressions reported in Ref. 16, we do not calculate the last term in Eq. (52) of Ref. 16, which actually vanishes for the reasons explained above. From first order perturbation theory applied to the Kohn and Sham equation, we get the change in the pseudowave functions due to the perturbation

$$(H^\sigma + Q^\sigma - \varepsilon_{i,\sigma} S)|\Delta^\mu \tilde{\psi}_{i,\sigma}\rangle = -\tilde{P}^\dagger_{c,\sigma}\left(\frac{dH^\sigma}{d\mu} - \varepsilon_{i,\sigma}\frac{\partial S}{\partial \mu}\right)|\tilde{\psi}_{i,\sigma}\rangle, \tag{11}$$

where the role of the operator Q^σ is explained in Ref. 1. $\frac{dH^\sigma}{d\mu}$ depends self-consistently on the first order derivatives of the charge densities. We have

$$\frac{dH^\sigma}{d\mu} = \frac{\partial H^\sigma}{\partial \mu} + \int d^3r \frac{d\tilde{V}^\sigma_{Hxc}(\mathbf{r})}{d\mu} K(\mathbf{r}) + \sum_{I,mn} \Delta D^{1,\sigma,\mu}_{I,mn} |\beta^I_m\rangle\langle\beta^I_n|, \tag{12}$$

where $\Delta D^{1,\sigma,\mu}_{I,mn} = (\frac{dD^{1,\sigma}_{I,mn}}{d\mu} - \frac{d\tilde{D}^{1,\sigma}_{I,mn}}{d\mu})$. Note that in Eq. (12), the derivative of $\tilde{V}^\sigma_{Hxc}(\mathbf{r})$ is done allowing the core charge to vary, while $\frac{\partial H^\sigma}{\partial \mu}$ is calculated at fixed wave functions and core charge and is given by

$$\frac{\partial H^\sigma}{\partial \mu} = \int d^3r \frac{\partial \tilde{V}_{\mathrm{loc}}(\mathbf{r})}{\partial \mu} K(\mathbf{r}) + \int d^3r \tilde{V}^\sigma_{\mathrm{eff}}(\mathbf{r}) \frac{\partial K(\mathbf{r})}{\partial \mu} + \sum_{I,mn} (D^{1,\sigma}_{I,mn} - \tilde{D}^{1,\sigma}_{I,mn}) \frac{\partial(|\beta^I_m\rangle\langle\beta^I_n|)}{\partial \mu}. \tag{13}$$

The partial derivatives of $D^{1,\sigma,\mu}_{I,mn}$ and $\tilde{D}^{1,\sigma,\mu}_{I,mn}$ which, rigorously speaking, would belong to the partial derivative of the Hamiltonian, are in $\Delta D^{1,\sigma,\mu}_{I,mn}$. This is relevant for the calculation of the forces (see below). $\Delta D^{1,\sigma,\mu}_{I,mn}$ are quantities that are calculated by integrals over the spheres and vanish in the US case. In the PAW case, we have

$$\frac{dD^{1,\sigma}_{I,mn}}{d\mu} = \sum_{\sigma_1} \int_{\Omega_I} d^3r \Phi^{I,AE}_m(\mathbf{r}) \Phi^{I,AE}_n(\mathbf{r}) \frac{dV^{I,\sigma}_{\mathrm{eff}}}{d\rho^{1,I}_{\sigma_1}} \frac{d\rho^{1,I}_{\sigma_1}}{d\mu}. \tag{14}$$

$\frac{d\tilde{D}^{1,\sigma}_{I,mn}}{d\mu}$ is calculated by a similar expression, putting $\tilde{V}^{I,\sigma}_{\mathrm{eff}}$ in the place of $V^{I,\sigma}_{\mathrm{eff}}$, $\tilde{\rho}^{1,I}_\sigma + \hat{\rho}^I_\sigma$ in the place of $\rho^{1,I}_\sigma$, and making an AE-PS substitution. If the partial derivatives of the PAW Hamiltonian are defined as in Eq. (13), the PAW and US forces have the same expression and are given (except for a minus sign) by Eq. (14) in Ref. 8

$$\frac{dE_{\mathrm{tot}}}{d\lambda} = \sum_{i\sigma} \langle\tilde{\psi}_{i,\sigma}|\frac{\partial H^\sigma}{\partial \lambda} - \varepsilon_{i,\sigma}\frac{\partial S}{\partial \lambda}|\tilde{\psi}_{i,\sigma}\rangle + \sum_\sigma \int d^3r_1 \tilde{V}^\sigma_{xc}(\mathbf{r}_1) \frac{\partial \tilde{\rho}_{c,\sigma}(\mathbf{r}_1)}{\partial \lambda}. \tag{15}$$

By deriving this expression with respect to μ, we obtain five terms for the second derivatives of the total energy. The first, second, fourth, and fifth PAW and US terms coincide and are given by Eqs. (39), (40), (42), and (35) in Ref. 8, provided that the screened coefficients of the nonlocal US-PP term $D^\sigma_{I,mn} + D^{(0),\gamma(I)}_{mn}$ (called D^σ_{Imn} in Ref. 8) are substituted by the PAW combination $D^\sigma_{I,mn} + D^{1,\sigma}_{I,mn} - \tilde{D}^{1,\sigma}_{I,mn}$ [where $D^\sigma_{I,mn} = \int d^3r \tilde{V}^\sigma_{\mathrm{eff}}(\mathbf{r}) \hat{Q}^I_{mn}(\mathbf{r} - \mathbf{R}_I)$ in both the US and the PAW cases]. For completeness, we rewrite here three of these four terms for an insulator. Equation (39) of Ref. 8 becomes

$$\frac{d^2E^{(1)}_{\mathrm{tot}}}{d\mu d\lambda} = \sum_{i,\sigma} \langle\tilde{\psi}_{i,\sigma}|\left[\frac{\partial^2 H^\sigma}{\partial \mu\, \partial \lambda} - \varepsilon_{i,\sigma}\frac{\partial^2 S}{\partial \mu\, \partial \lambda}\right]|\tilde{\psi}_{i,\sigma}\rangle, \tag{16}$$

Equation (40) of Ref. 8 is

$$\frac{d^2E^{(2)}_{\mathrm{tot}}}{d\mu d\lambda} = 2\,\mathrm{Re}\sum_{i,\sigma} \langle\Delta^\mu\tilde{\psi}_{i,\sigma}|\left[\frac{\partial H^\sigma}{\partial \lambda} - \varepsilon_{i,\sigma}\frac{\partial S}{\partial \lambda}\right]|\tilde{\psi}_{i,\sigma}\rangle. \tag{17}$$

Equation (42) of Ref. 8 becomes

$$\frac{d^2E^{(4)}_{\mathrm{tot}}}{d\mu d\lambda} = -\sum_{i,\sigma}\left\{\langle\delta^\mu\tilde{\psi}_{i,\sigma}|\left[\frac{\partial H^\sigma}{\partial \lambda} - \varepsilon_{i,\sigma}\frac{\partial S}{\partial \lambda}\right]|\tilde{\psi}_{i,\sigma}\rangle + (\mu \leftrightarrow \lambda)\right\}. \tag{18}$$

The term due to the explicit treatment of the core charge [Eq. (35) in Ref. 8] has been discussed in several papers and does not change in the present scheme.

The third term, which in the US case is given by Eq. (41) in Ref. 8,

$$\frac{d^2E^{(3)\mathrm{US}}_{\mathrm{tot}}}{d\mu d\lambda} = \sum_\sigma \int d^3r \frac{d\tilde{V}^\sigma_{Hxc}(\mathbf{r})}{d\mu} \Delta^\lambda[\tilde{\rho}_\sigma(\mathbf{r}) + \hat{\rho}_\sigma(\mathbf{r})], \tag{19}$$

has an additional contribution in the PAW case. In both schemes, this term is given by

$$\frac{d^2E^{(3)}_{\mathrm{tot}}}{d\mu d\lambda} = \sum_{i,\sigma} \langle\tilde{\psi}_{i,\sigma}|\frac{d}{d\mu}\left(\frac{\partial H^\sigma}{\partial \lambda}\right) - \frac{\partial^2 H^\sigma}{\partial \mu\, \partial \lambda}|\tilde{\psi}_{i,\sigma}\rangle - \sum_{i,\sigma} \langle\tilde{\psi}_{i,\sigma}|\left(\frac{dH^\sigma}{d\mu} - \frac{\partial H^\sigma}{\partial \mu}\right)|\delta^\lambda\tilde{\psi}_{i,\sigma}\rangle, \tag{20}$$

but, in the PAW case, both the difference $\frac{dH^\sigma}{d\mu} - \frac{\partial H^\sigma}{\partial \mu}$, given by Eq. (12), and the difference

$$\frac{d}{d\mu}\left(\frac{\partial H^\sigma}{\partial \lambda}\right) - \frac{\partial^2 H^\sigma}{\partial \mu\, \partial \lambda} = \int d^3r \frac{d\tilde{V}^\sigma_{Hxc}(\mathbf{r})}{d\mu} \frac{\partial K(\mathbf{r})}{\partial \lambda} + \sum_{I,mn} \Delta D^{1,\sigma,\mu}_{I,mn} \frac{\partial(|\beta^I_m\rangle\langle\beta^I_n|)}{\partial \lambda}, \tag{21}$$

contain a contribution calculated inside the spheres. Collecting all terms, $\frac{d^2E^{(3)}_{\mathrm{tot}}}{d\mu d\lambda}$ can be rewritten in a compact form by adding to Eq. (19) a term that vanishes in the US case and characterizes the PAW scheme

$$\frac{d^2E^{(3)}_{\mathrm{tot}}}{d\mu d\lambda} = \frac{d^2E^{(3)\mathrm{US}}_{\mathrm{tot}}}{d\mu d\lambda} + \sum_\sigma \sum_{I,mn} \Delta D^{1,\sigma,\mu}_{I,mn} b^{\sigma,\lambda}_{I,mn}. \tag{22}$$

$\Delta D^{1,\sigma,\mu}_{I,mn}$ appears in Eq. (12) and is calculated at each iteration in order to get the self-consistent solutions of the linear system [Eq. (11)]. $b^{\sigma,\lambda}_{I,mn}$ needed also in Eq. (9) is already available. Equation (22) is not exactly equivalent to Eq. (80) in Ref. 16 because, according to Eq. (22), $\frac{d\tilde{V}^\sigma_{Hxc}(\mathbf{r})}{d\mu}$ to be inserted in $\frac{d^2E^{(3)\mathrm{US}}_{\mathrm{tot}}}{d\mu d\lambda}$ is the same in the US and PAW approaches while, according to Ref. 16, a more complex expression should be used in the latter case. After this change, Eq. (22) becomes equivalent to Eq. (80) in Ref. 16, but it is written in a form that does not require any new integral over the spheres. Moreover, when λ is an electric field, $b^{\sigma,\lambda}_{I,mn}$ vanishes. Hence,

TABLE I. Calculated geometries (d) and harmonic vibrational frequencies (ω) of CO and H_2O. The present PAW results are compared with experiment and previous calculations with localized basis sets.

	PAW-LDA	Other-theory (LDA)	PAW-PBE	Other-theory (PBE)	Expt.
CO					
d (Å)	1.129	1.128[a]	1.136	1.134[e]	1.128[f]
ω_Σ (cm^{-1})	2173	2176[a]	2129	2123[e]	2170[f]
H_2O					
d (Å)	0.972	0.970,[b] 0.971,[a] 0.979[c]	0.971	0.970,[e] 0.971[b]	0.957[b]
α	105.0	104.9,[b] 105.9[c]	104.2	104.2,[e] 104.1[b]	104.5[b]
ω_{A_1} (cm^{-1})	1542	1560,[b] 1534,[d] 1547,[a] 1502[c]	1590	1593,[e] 1601[b]	1648[b]
ω_{A_1} (cm^{-1})	3704	3729,[b] 3698,[d] 3714,[a] 3725[c]	3700	3697,[e] 3702[b]	3832[b]
ω_{B_2} (cm^{-1})	3815	3835,[b] 3812,[d] 3823,[a] 3848[c]	3807	3801,[e] 3804[b]	3943[b]

[a]Reference 30.
[b]Reference 32.
[c]Reference 34 (US-PPs).
[d]Reference 33.
[e]Reference 29.
[f]Reference 28.

the US and PAW expressions of the dielectric tensor,[20,21] as well as of the BEC calculated from the polarization induced by atomic displacements, coincide. However, the PAW contribution is required for the dynamical matrix or for the BEC calculated from the forces induced by an electric field. The linear system, Eq. (11), has always a PAW contribution and must be modified with respect to the US case. The above expressions have been implemented in the QUANTUM-ESPRESSO (Ref. 22) package (QE) in which the PAW ground state,[23] as well as DFPT (Refs. 1 and 2) for US-PPs,[8,9,20,24] were already available.

III. APPLICATIONS

In the following, we validate the above formulas by three examples: two molecules (CO and H_2O) and ferromagnetic bcc-Fe. We use the local density approximation (LDA),[25] and the generalized gradient approximation (GGA) (Ref. 26) in the spin unpolarized form for the two molecules and in the spin-polarized form for bcc-Fe. The PAW data sets of Fe, C, O, and H are described in the note.[27] The kinetic energy cutoffs for the wave functions are 50 Ry, for CO and H_2O and 45 Ry for bcc-Fe. The cutoff for the charge density is 300 Ry. These cutoffs give frequencies converged within 3 cm^{-1}. For the two molecules, we used a box of 20 a.u. and we sampled the BZ with the Γ point, while for bcc-Fe, we used a $16\times16\times16$ uniform **k**-point grid (a smearing parameter $\sigma=0.02$ Ry) and calculated the dynamical matrices in a $4\times4\times4$ **q**-point grid. A Fourier interpolation is then used to obtain the phonon frequencies in the other points of the BZ.

In Table I, we report the calculated geometries and harmonic vibrational frequencies of the two molecules comparing them with experiments and with a few selected previous calculations. We start with the CO molecule. Experimentally, the CO molecule has an infrared absorption peak at 2143 cm^{-1} but this frequency, influenced by anharmonicity, cannot be directly compared with our value obtained within the harmonic approximation. Subtracting anharmonic effects, the experimental harmonic CO stretch frequency can be estimated to be 2170 cm^{-1}.[28] Our DFPT LDA (GGA) value is 2173 (2129) cm^{-1} at the equilibrium distance $d=2.134$ (2.147) a.u. (experiment 2.132 a.u.).[28] Both our LDA and GGA values are in good agreement with previous all-electron calculations which employed localized basis sets.[29,30] In order to validate our implementation of DFPT with PAW, we recalculated the CO stretch frequency by a "frozen phonon" technique. The forces induced on C and O by displacements of ±0.002, ±0.001 a.u. were fitted by a third order polynomial. Using the coefficient of the linear term of the polynomial as the interatomic force constant, we obtained frequencies differing less than 0.5 cm^{-1} from the DFPT result in both the LDA and the GGA cases.[31] We checked also the importance of the PAW corrections in Eq. (12) and in Eq. (22), by calculating the CO stretch frequency neglecting the contribution of the change in the nonlocal PP coefficients, that is by taking $\Delta D^{1,\sigma,\mu}_{I,mn}=0$, and we found 2165 (2119) cm^{-1}. Thus, in CO, the change in the coefficients of the nonlocal PP, whose actual values are PP dependent, gives a small, but not negligible correction.

As a second example, we consider a water molecule. The experimental vibrational frequencies of this molecule, taken from Table II of Ref. 32, are (in parenthesis the values corrected for anharmonicity): $\omega_{A_1}=1595$ (1648) cm^{-1}, $\omega_{A_1}=3657$ (3832) cm^{-1}, $\omega_{B_2}=3756$ (3943) cm^{-1}. The experimental geometry is $d_{OH}=1.808$ a.u. and $\alpha=104.5°$. We find a LDA (GGA) equilibrium geometry, $d_{OH}=1.837$ (1.834) a.u. and $\alpha=105.0$ (104.2°), and harmonic vibrational frequencies $\omega_{A_1}=1542$ (1590) cm^{-1}, $\omega_{A_1}=3704$ (3700) cm^{-1}, and $\omega_{B_2}=3815$ (3807) cm^{-1}. On average, the theoretical values differ of 121 (109) cm^{-1} from experiment but are in good

agreement with previous theoretical results reported in Table I. For instance, in the LDA case, the average difference with the US-PP result of Ref. 34 is 31 cm^{-1}. The differences with the localized basis results of Refs. 30, 32, and 33 are 21, 8, and 8 cm^{-1}, respectively. In the GGA case, there is an average difference of 4 and 5 cm^{-1} with Refs. 29 and 32. Actually our results are influenced by the TE error of the PAW data set. We have estimated this error by recalculating, in the LDA case, the frequencies with a PAW data set with O core radii $r_s=1.2$ a.u., $r_p=1.2$ a.u., $r_d=1.1$ a.u., the same reference energies reported in the note[27] and a wave functions cutoff of 60 Ry. With these parameters, the equilibrium geometry is $d_{OH}=1.836$ a.u. and $\alpha=104.9°$, and the three frequencies are $\omega_{A_1}=1547$ cm^{-1}, $\omega_{A_1}=3711$ cm^{-1}, and $\omega_{B_2}=3820$ cm^{-1}. We can therefore estimate an average TE uncertainty of at least 6 cm^{-1}. The accuracy of the PAW DFPT implementation has been tested also by comparing the DFPT results with a "frozen phonon" calculation. We took displacements of ± 0.002, and ± 0.001 a.u. and fitted the induced atomic forces with third order polynomials. Diagonalizing the dynamical matrix obtained from the linear terms of the polynomials we obtained frequencies that differ less than 1 cm^{-1} from the DFPT result both in the LDA and in the GGA cases.[31] In order to obtain this kind of agreement, it is essential to include the PAW corrections. Actually, as for CO, we estimated their effects setting $\Delta D^{1,\sigma,\mu}_{I,mn}=0$ and obtained $\omega_{A_1}=1539$ (1588) cm^{-1}, $\omega_{A_1}=3690$ (3685) cm^{-1}, and $\omega_{B_2}=3813$ (3804) cm^{-1}, and hence an average difference of 6 (6) cm^{-1}.

As a third example, we consider the phonon dispersions of bcc-Fe. We started by validating the DFPT PAW code at finite **q** vectors. We have calculated the three degenerate frequencies of bcc-Fe at the $H=\frac{2\pi}{a_0}(1,0,0)$ point by three different methods: a DFPT calculation at the H point of BZ of the bcc-lattice, a DFPT calculation at the Γ point of the BZ of the conventional cubic cell, a "frozen phonon" calculation in which we displaced the two atoms in the conventional cubic cell along the x direction: one atom in $a_0(u,0,0)$ and the other in $a_0(1/2-u,1/2,1/2)$. Using a $16\times16\times16$ **k**-point mesh for the cubic cell and a $20\times20\times20$ mesh for the bcc cell, at $a_0=5.38$ a.u., we obtained 295 cm^{-1} with all the three methods and differences among them smaller than 0.5 cm^{-1}.

In Fig. 1, we compare the PAW dispersions with the inelastic neutron scattering data.[35] The experimental data are taken at $T=295$ K and the PAW dispersions are calculated at the theoretical equilibrium lattice constant corrected for the thermal lattice expansion ($a_0=5.36+0.02$ a.u., experiment $a_0=5.42$ a.u.). With the present PAW data set the theoretical bulk modulus is $B=1930$ kbar (experiment $B=1680$ kbar) and the magnetic moment is $\mu_0=2.18\mu_B$ (experiment $\mu_0=2.22\mu_B$). When compared to experiment, the present dispersions have the same quality of previous published results.[36–38] Actually, the agreement is quite good with the PAW results of Ref. 36 that are calculated at room temperature. The dispersions of Ref. 37, calculated with US-PPs, although similar to the present PAW result cannot be directly compared because they are calculated neglecting thermal expansion. In Fig. 1, we report the dispersions calculated with the US-PP used in Ref. 37 at its theoretical lattice constant ($a_0=5.40$ a.u., $B_0=1520$ kbar) and at the lattice constant expanded for thermal effects ($a_0=5.42$ a.u., $\mu_0=2.42\mu_B$). Comparing the phonons at room temperature, there are some discrepancies between the two calculations. With respect to the US-PPs results, PAW improves the agreement with experiment for some branches, for instance, for the longitudinal acoustic mode along $\Gamma-N$, while in other cases, it is of similar quality or slightly worse. Presently, the reason of these differences is not completely clear. In the present US-PP calculation we use the same cut-off energy for the wave functions and **k**-point sampling as in the PAW calculation, and 400 Ry for the charge density cutoff, so numerical convergence is ruled out. Magnetism has a huge effect on these dispersions because nonmagnetic bcc-Fe is unstable and also small changes in the lattice constant will affect the phonon dispersions so a PP TE that gives only small differences in the lattice constant or on the magnetic moment could lead to visible differences in the phonon dispersions. We exclude that the reason of the difference is an intrinsic TE of the US-PPs. Actually, making an US-PP with the same recipe as the PAW data set[27] gives (at the theoretical lattice constant corrected for thermal expansion $a_0=5.36+0.02$ a.u.) phonon dispersions that are indistinguishable from the PAW result in Fig. 1 with a bulk modulus $B=1880$ kbar and a magnetic moment $\mu_0=2.21\mu_B$.

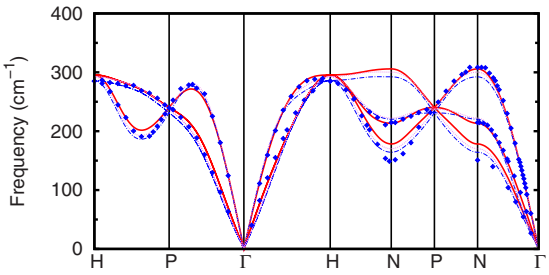

FIG. 1. (Color online) Calculated PAW phonon dispersions (solid lines) for ferromagnetic bcc-Fe compared to inelastic neutron scattering data at $T=295$ K (diamonds) (Ref. 35). Dispersions calculated with the US-PP of Ref. 37 at the theoretical lattice constant ($a_0=5.40$ a.u.) (dotted line) and at the lattice constant expanded to account for thermal effects ($a_0=5.42$ a.u.) (dot-dashed line) are also shown.

In conclusion, we have shown how to generalize DFPT to the PAW method. We have found that only minor additions to DFPT for US-PPs are sufficient to make it work within PAW. We have validated the theory by a comparison of DFPT with a "frozen phonon" approach in CO, H_2O and ferromagnetic bcc-Fe. We have found that the PAW corrections are usually small, but are necessary to make DFPT to agree within 1 cm^{-1} with the "frozen phonon" results.

ACKNOWLEDGMENTS

The work was sponsored by MIUR PRIN/Cofin Contracts under Grant No. 2006022847 as well as by INFM/CNR "Iniziativa transversale calcolo parallelo." The calculations have been done on the SISSA Linux cluster and GRID and at CINECA in Bologna.

[1] S. Baroni, P. Giannozzi, and A. Testa, Phys. Rev. Lett. **58**, 1861 (1987); S. Baroni, S. de Gironcoli, A. Dal Corso, and P. Giannozzi, Rev. Mod. Phys. **73**, 515 (2001).
[2] P. Giannozzi, S. de Gironcoli, P. Pavone, and S. Baroni, Phys. Rev. B **43**, 7231 (1991).
[3] S. Y. Savrasov and D. Y. Savrasov, Phys. Rev. B **54**, 16487 (1996).
[4] J.-H. Lee, Y.-C. Hsue, and A. J. Freeman, Phys. Rev. B **73**, 172405 (2006).
[5] X. Gonze, D. C. Allan, and M. P. Teter, Phys. Rev. Lett. **68**, 3603 (1992).
[6] R. Heid and K.-P. Bohnen, Phys. Rev. B **60**, R3709 (1999).
[7] D. Vanderbilt, Phys. Rev. B **41**, 7892 (1990).
[8] A. Dal Corso, Phys. Rev. B **64**, 235118 (2001).
[9] A. Dal Corso, Phys. Rev. B **76**, 054308 (2007).
[10] J. Paier, R. Hirschl, M. Marsman, and G. Kresse, J. Chem. Phys. **122**, 234102 (2005).
[11] J. Paier, M. Marsman, and G. Kresse, J. Chem. Phys. **127**, 024103 (2007).
[12] A. Dal Corso, J. Phys.: Condens. Matter **20**, 445202 (2008).
[13] P. E. Blöchl, Phys. Rev. B **50**, 17953 (1994).
[14] G. Kresse and D. Joubert, Phys. Rev. B **59**, 1758 (1999).
[15] C. Audouze, F. Jollet, M. Torrent, and X. Gonze, Phys. Rev. B **73**, 235101 (2006).
[16] C. Audouze, F. Jollet, M. Torrent, and X. Gonze, Phys. Rev. B **78**, 035105 (2008).
[17] To simplify the notation, in this paper, we give only the expressions for insulators.
[18] The composite index L explained in Ref. 14 is omitted here, although it is used in the code.
[19] The derivatives of this term do not change in the present approach and are not discussed in the paper.
[20] J. Tóbik and A. Dal Corso, J. Chem. Phys. **120**, 9934 (2004).
[21] M. Gajdoš, K. Hummer, G. Kresse, J. Furthmüller, and F. Bechstedt, Phys. Rev. B **73**, 045112 (2006).
[22] P. Giannozzi *et al.*, J. Phys.: Condens. Matter **21**, 395502 (2009) See http://www.quantum-espresso.org
[23] I started from the ground state PAW implementation present in QE version 4.0.3, due to L. Paulatto, S. de Gironcoli, G. Fratesi, and R. Mazzarello (unpublished).
[24] US-PPs BEC are due to G. Deinzer and S. de Gironcoli (unpublished).
[25] J. P. Perdew and A. Zunger, Phys. Rev. B **23**, 5048 (1981).
[26] J. P. Perdew, K. Burke, and M. Ernzerhof, Phys. Rev. Lett. **77**, 3865 (1996).
[27] PAW PPs have been generated with the valence electronic configurations: $1s^2$ (H), $2s^2 2p^2$ (C), $2s^2 2p^4$ (O), $3d^{6.5} 4s^{1.5}$ (Fe). The core radii (in Bohr a.u.) are: H $r_s=1.0$, $r_p=0.75$ (p is local), C $r_s=1.3$, $r_p=1.45$, $r_d=1.1$ (d is local), O $r_s=1.35$, $r_p=1.35$, $r_d=1.3$ (d is local), Fe $r_s=2.2$, $r_p=2.2$, $r_d=1.8$. The nonlocal channels are fitted at the eigenvalue and at $\epsilon=0.05$ Ry in H, C, and O and at $\epsilon=6.3$ Ry (s), $\epsilon=6.5$ Ry (p) in Fe. The unbound d channel at $\epsilon=0.10$ (0.15) [−0.3] Ry in C (O) [Fe]. NLCC is used in C, O, and Fe ($r_c=0.8, 0.7, 1.2$). In Fe the local potential is the all-electron potential smoothed before $r=2.1$ a.u.. PAW-PPs are generated by the ld1 atomic code using a PAW implementation due mainly to G. Fratesi *et al.* (unpublished).
[28] B. G. Johnson, P. M. W. Gill, and J. A. Pople, J. Chem. Phys. **98**, 5612 (1993).
[29] Data have been taken from the NIST-CCCB (http://cccbdb.nist.gov/). The theoretical frequencies have been obtained by using the *aug-cc-pVTZ* basis.
[30] A. Briley, M. R. Pederson, K. A. Jackson, D. C. Patton, and D. V. Porezag, Phys. Rev. B **58**, 1786 (1998).
[31] Note that in QE, the printed forces are corrected so that the total force vanishes exactly. In the frozen phonon test this correction has not been used and the dynamical matrix has not been corrected to impose the acoustic sum rule.
[32] X. Xu and W. A. Goddard, J. Phys. Chem. A **108**, 2305 (2004).
[33] D. Porezag and M. R. Pederson, Phys. Rev. B **54**, 7830 (1996).
[34] P. Umari, X. Gonze, and A. Pasquarello, Phys. Rev. B **69**, 235102 (2004).
[35] B. N. Brockhouse, H. E. Abou-Helal, and E. D. Hallman, Solid State Commun. **5**, 211 (1967).
[36] F. Körmann, A. Dick, B. Grabowski, B. Hallstedt, T. Hickel, and J. Neugebauer, Phys. Rev. B **78**, 033102 (2008).
[37] A. Dal Corso and S. de Gironcoli, Phys. Rev. B **62**, 273 (2000).
[38] D. Alfè, G. Kresse, and M. J. Gillan, Phys. Rev. B **61**, 132 (2000).